

# *In vivo* tumor diagnosis and photodynamic therapy *via* tumoral pH-responsive polymeric micelles†

Heebeom Koo,‡<sup>a</sup> Hyejung Lee,‡<sup>ab</sup> Sojin Lee,<sup>ac</sup> Kyung Hyun Min,<sup>ab</sup> Min Sang Kim,<sup>d</sup> Doo Sung Lee,<sup>d</sup> Yongseok Choi,<sup>c</sup> Ick Chan Kwon,<sup>a</sup> Kwangmeyung Kim\*<sup>a</sup> and Seo Young Jeong\*<sup>b</sup>

Received 14th May 2010, Accepted 25th June 2010

DOI: 10.1039/c0cc01413c

**We report protoporphyrin IX (PpIX) encapsulated pH-responsive micelles for cancer treatment. This system showed pH-responsive micellization/demicellization transition at tumoral acidic pH and enabled *in vivo* tumor diagnosis and therapy simultaneously.**

In recent decades, photodynamic therapy (PDT) using photosensitizers has been receiving considerable interest as a potential treatment of prostate, skin and lung cancers.<sup>1</sup> After injection and upon irradiation with an appropriate wavelength, the photosensitizers produce singlet oxygen which causes damage to adjacent tissues.<sup>2</sup> PDT can effectively and non-invasively treat diseased tissues containing photosensitizers, while causing minimal nonspecific damage to other tissues.<sup>3</sup> Moreover, photosensitizers could be useful in both diagnosis and therapy, because upon irradiation, they produce strong fluorescence and singlet oxygen simultaneously without additional fluorescent dye.<sup>4</sup> But, the hydrophobicity of photosensitizers and the low selectivity to target sites often limit the clinical utility of PDT.<sup>5</sup>

To overcome these difficulties, various nano-sized materials like nanospheres, liposomes, polymer–drug conjugates, and polymeric micelles have been developed and showed the possibilities of successful delivery of photosensitizers.<sup>6</sup> When systemically injected, they exhibit prolonged circulation by avoiding rapid renal clearance and unwanted uptake by the reticuloendothelial system (RES), and this results in enhanced permeability and retention (EPR) in tumor tissues with defective vascular architecture.<sup>7</sup> Among them, stimuli-responsive polymeric micelles show even more specific delivery to target sites by controlled release of molecules upon stimuli like temperature<sup>8</sup> or pH.<sup>9</sup>

The extracellular pH of tumor tissues is about 6.4–6.8, lower than that of normal tissue (pH 7.4), that is caused by

up-regulated glycolysis producing lactates and protons in extracellular environments.<sup>10</sup> This lower pH of tumor tissue can be targeted for therapeutic strategies in drug delivery and biomedical imaging.<sup>11</sup> Many block copolymer micelles controlled by pH have been developed for drug delivery and showed attractive pH-responsive character.<sup>12</sup> But large amounts of them were responsive to endosomal or lysosomal pH, and a few of them were targeted to extracellular pH in tumor tissue.<sup>13</sup>

Therefore, in previous reports, we have described the pH-responsive MPEG poly( $\beta$ -amino ester) polymeric micelles, and these micelles showed sharp pH-dependent demicellization at the acidic extracellular pH of tumors, because the tertiary amine groups in the hydrophobic amino ester block are protonated and become hydrophilic in acidic pH below 6.5.<sup>14</sup> We expected that this tumor targeted delivery system would have great potential in PDT. At a tumor site, photosensitizer could be released as demicellization and produce fluorescence and singlet oxygen for simultaneous diagnosis and therapy (Fig. 1).<sup>15</sup>

To fabricate the pH-responsive block copolymer micelles, we combined hydrophilic MPEG with poly( $\beta$ -amino ester), since the latter is pH-sensitive due to its tertiary amines ( $pK_b = 6.5$ ).<sup>14</sup> It was prepared by a Michael-type polymerization and confirmed using <sup>1</sup>H-NMR and GPC.<sup>16</sup> The average molecular weight of MPEG–poly( $\beta$ -amino ester) block copolymer was 17.4 kDa and its polydispersity was about 1.3. Protoporphyrin IX (PpIX), a hydrophobic synthesizer, was loaded into these polymeric micelles by a solvent evaporation method.<sup>17</sup> When the PpIX content in the polymeric micelles was less than 10 wt%, the drug-loading efficiency was about 70–80%. However, there was a marked decrease in the loading

<sup>a</sup> Biomedical Research Center, Korea Institute of Science and Technology, Seongbuk-Gu, Seoul 136-791, South Korea. E-mail: kim@kist.re.kr; Fax: (+82) 2-958-5909; Tel: (+82) 2-958-5912

<sup>b</sup> Department of Life and Nanopharmaceutical Science, Kyung Hee University, 1 Hoegi-dong, Dongdaemun-gu, Seoul 130-701, South Korea. E-mail: syjeong@khu.ac.kr; Fax: (+82) 2-966-3885; Tel: (+82) 2-961-9254

<sup>c</sup> School of Life Science and Biotechnology, Korea University, 1 Anam-dong, Seongbuk-gu, Seoul 136-701, South Korea

<sup>d</sup> Department of Polymer Science and Engineering, Sungkyunkwan University, Suwon 440-746, South Korea

† Electronic supplementary information (ESI) available: Synthesis and characterization of the polymers and micelles. The images of cells and mice. See DOI: 10.1039/c0cc01413c

‡ These authors contributed equally to this work.

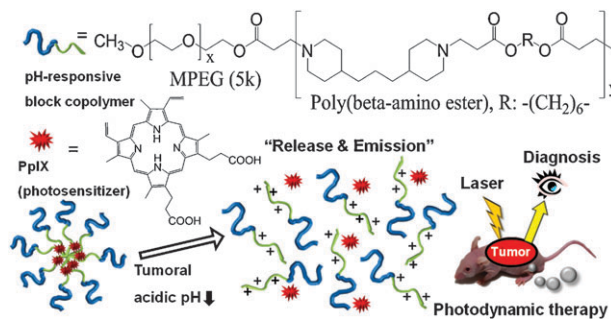


**Fig. 1** The micellization/demicellization transition of PpIX loaded tumoral pH-responsive micelles and *in vivo* simultaneous tumor diagnosis and photodynamic therapy by this system.

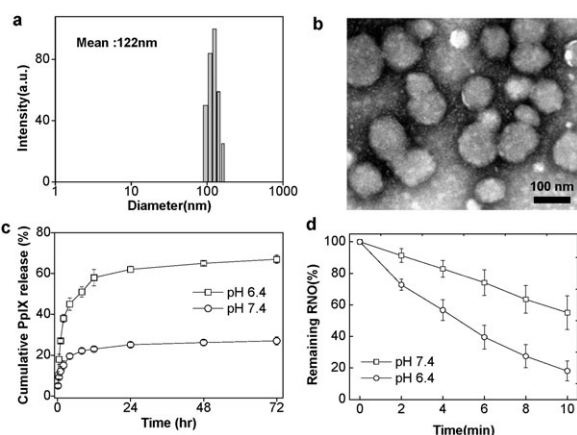


**Fig. 2** Characteristics of PpIX-pH-PMs. (a) The size distribution of micelles by dynamic light scattering (DLS). (b) Transmission electron microscopy (TEM) images. (c) *In vitro* PpIX release from the micelles at pH 6.4 and pH 7.4. (d) Singlet oxygen generation detected by using RNO as a sensor according to irradiation time. Results represent means  $\pm$  s.e. ( $n = 5$ ).

efficiency (to less than 50%) when the drug was present at 20 wt%. (Table S1 in ESI†).<sup>14b</sup> Based on light scattering experiments, the average size of the PpIX-loaded pH-responsive polymeric micelles (PpIX-pH-PMs) was about 122 nm with a narrow size distribution, which was greater than that of the unloaded micelles (42 nm), indicating that PpIX molecules were trapped in the hydrophobic inner cores and increased the average size of micelles (Fig. 2(a) and Fig. S1 in ESI†). TEM images showed that these micelles were nearly spherical (Fig. 2(b)).

The pH-dependent PpIX release profile from the PpIX-pH-PMs was investigated by dialysis (Fig. 2(c)). At pH 7.4, the total amount of release was only about 23% for 1 day, showing that they maintained micellar structures under physiological conditions. However, the PpIX release rate from micelles at lower pH (pH 6.4) was much faster, with about 60% released within 6 h, indicating that PpIX-pH-PMs rapidly demicellized and released drug in weakly acidic environments.

We also measured singlet oxygen generation using *p*-nitrosodimethylaniline (RNO) as singlet oxygen sensor (Fig. 2(d)).<sup>18</sup> During irradiation, the decrease of absorbance at 400 nm indicated generation of singlet oxygen as a function of the time of He–Ne laser exposure. When we irradiated PpIX-pH-PMs with the laser, optical density decreased even more rapidly at pH 6.4 than 7.4, showing that the amount of singlet oxygen from micelles highly increased at tumoral pH.

The intracellular localization of free PpIX and PpIX-pH-PMs was investigated using confocal microscopy, based on the fluorescence of PpIX itself (Fig. 3). When SCC7 cells were incubated with free PpIX, cellular uptake of PpIX molecules was not different at both pH 6.4 and pH 7.4. In the case of PpIX-pH-PMs at pH 7.4, weak fluorescence was detected at cell membranes, suggesting that PpIX molecules were slowly released from micelles at physiological pH. But at pH 6.4, a very strong fluorescence signal of PpIX was observed in the cytoplasm, compared to that at pH 7.4. This pH dependent cellular uptake of PpIX molecules is due to the

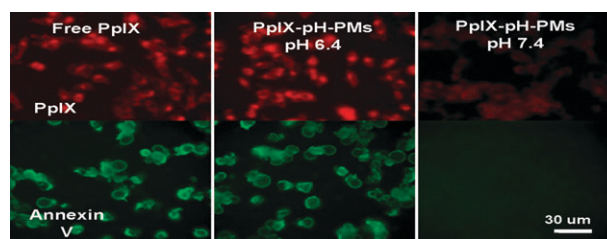


**Fig. 3** Cellular uptake and photocytotoxicity of free PpIX and PpIX-pH-PMs against SCC7 cells observed by confocal laser scanning microscope. Fluorescence images of PpIX were obtained with a TRITC filter set (red), Annexin V-FITC stain (green) depicts apoptotic cells.

rapid demicellization of PpIX-pH-PMs under weakly acidic extracellular conditions, leading to the rapid release of PpIX from polymeric micelles and subsequent internalization into cells. To determine phototoxicity of PpIX-pH-PMs, we washed these cells with PBS, and irradiated them with a He–Ne laser. Before irradiation, we observed no cytotoxicity in all cells (Fig. S2 in ESI†). But after irradiation, cells treated with free PpIX or PpIX-pH-PMs at pH 6.4 showed apoptosis with the Annexin V-FITC treatment.<sup>19</sup> Because this block copolymer did not present any cytotoxicity in the cell culture system, we could say that this toxicity originated from singlet oxygen generation.<sup>20</sup> These data suggested that PpIX-pH-PMs were suitable for targeting to the acidic extracellular environments of tumors.

Next, we determined the tumor specificity of free PpIX and PpIX-pH-PMs non-invasively in live SCC7 tumor-bearing mice, also based on the fluorescence of PpIX. After *i.v.* injection of free PpIX and PpIX-pH-PMs, we monitored the time dependent biodistribution of free PpIX and PpIX-loaded polymeric micelles (Fig. 4(a)). In the case of free PpIX, strong fluorescent signals were mainly observed in livers and this signal was maintained for 24 h, indicating that the injected free PpIX was mainly accumulated in livers. These mice presented a very weak fluorescent signal in tumors and the tumors could not be clearly distinguished from the body, indicating that free PpIX was not accumulated efficiently in tumors. In the case of PpIX-pH-PMs, after 1 day post-injection, there was very strong fluorescence intensity at tumors. The tumors could be delineated from the surrounding background tissue, indicating the tumor targeted delivery of PpIX. In addition, the total photon counts in tumor tissue of PpIX-pH-PMs at 48 h post-injection were 10 fold higher than that of free PpIX every time (Fig. 4(b)). Upon *ex vivo* imaging of excised organs (liver, lung, spleen, kidney, heart) and tumors (Fig. 4(c)), PpIX-pH-PMs treated mice also showed the strongest fluorescent intensity in tumors, and PpIX uptake in other normal organs was not shown except in liver and kidney where PpIX was rapidly metabolized. This indicated that PpIX was successfully delivered to the tumors, and these highly sensitive fluorescent images of tumors in the whole body could give useful information for further clinical treatments.

In the same *in vivo* conditions, we also evaluated antitumor therapeutic efficacy of PpIX-pH-PMs. One day after injection, we treated the animals with 633 nm light ( $3 \text{ mW cm}^{-2}$ ) twice for 30 min. After 1 day, PpIX-pH-PMs treated mice showed

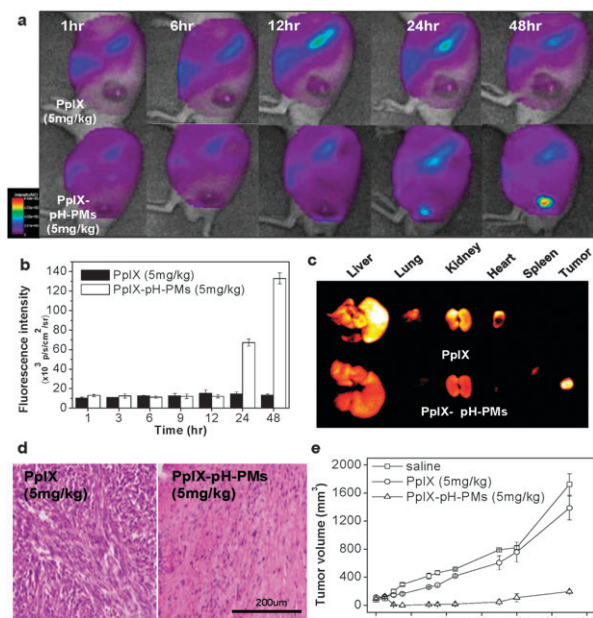


**Fig. 4** *In vivo* non-invasive fluorescent imaging and photodynamic therapy with PpIX-pH-PMs in tumor bearing mice. (a) Time-dependent whole body imaging of mice bearing SCC7 tumors after i.v. injection. (b) Quantification of *in vivo* tumor target specificity of free PpIX and PpIX-pH-PMs. Results represent means  $\pm$  SDs. ( $n = 3$ ). (c) *Ex vivo* images of organs (liver, lung, spleen, kidney and heart) and tumors. (d) H&E staining of tumor tissues 10 days after treatment. (e) Tumor growth of SCC7 tumor-bearing mice treated with drug injection and irradiation. Results represent means  $\pm$  SDs. ( $n = 2$ ).

hemorrhage where the laser was administered, and these indicate a large amount of PpIX was localized in tumors and produced cytotoxic singlet oxygen that induced tissue damage upon irradiation (Fig. S3 in ESI†). After 10 days, we sacrificed the mice, harvested tumor tissues, and performed histological examination (H&E staining) (Fig. 4(d)). In mice treated with PpIX-pH-PMs, most tumor cells were severely damaged or destroyed. But, in the case of free PpIX, there was incomplete cell death. The tumor growth graph also showed substantial evidence of successful therapy with PpIX-pH-PMs in tumor bearing mice (Fig. 4(e)).

In summary, we showed that pH-responsive polymeric micelles could efficiently deliver hydrophobic photosensitizer, PpIX to tumors *in vivo*. These micelles formed stable nano-sized structures suitable for the EPR effect, showed marked pH-responsive demicellization and released PpIX at weakly acidic tumoral conditions. In tumor bearing mice, these micelles showed clear fluorescent imaging of tumors and complete ablation of them. Therefore we can conclude that the combination of pH-responsive micelle and photosensitizer enables both tumor diagnosis and therapy simultaneously, and has great potential for biological studies and clinical treatments of various tumors.

This research was financially supported by the Real-Time Molecular Imaging Project (20100002043), the Global Research Laboratory Project of MEST (K20704000002-09A0500-00210), BK21 BNT Scientist Renovating for the

Drug Development Coping with Aged Society (2009K001594, 2009K001595) and the Intramural Research Program of the KIST.

## Notes and references

- (a) L. K. Folkes and P. Wardman, *Cancer Res.*, 2003, **63**, 776–779; (b) B. A. Standish, K. K. C. Lee, X. Jin, A. Mariampillai, N. R. Munce, M. F. G. Wood, B. C. Wilson, I. A. Vitkin and V. X. D. Yang, *Cancer Res.*, 2008, **68**, 9987–9995.
- H. Koizumi, Y. Kimata, Y. Shiraishi and T. Hirai, *Chem. Commun.*, 2007, 1846–1848.
- C. Fabris, G. Valduga, G. Miotto, L. Borsetto, G. Jori, S. Garbisa and E. Reddi, *Cancer Res.*, 2001, **61**, 7495–7500.
- S. J. Lee, K. Park, Y.-K. Oh, S.-H. Kwon, S. Her, I.-S. Kim, K. Choi, S. J. Lee, H. Kim, S. G. Lee, K. Kim and I. C. Kwon, *Biomaterials*, 2009, **30**, 2929–2939.
- Y. N. Konan, R. Gurny and E. Allémann, *J. Photochem. Photobiol., B*, 2002, **66**, 89–106.
- (a) N. Nishiyama, Y. Morimoto, W.-D. Jang and K. Kataoka, *Adv. Drug Delivery Rev.*, 2009, **61**, 327–338; (b) D. Brevet, M. Gary-Bobo, L. Raehm, S. Richeter, O. Hocine, K. Amro, B. Looock, P. Couleaud, C. Frochot, A. Morere, P. Maillard, M. Garcia and J.-O. Durand, *Chem. Commun.*, 2009, 1475–1477; (c) Y.-P. Fang, Y.-H. Tsai, P.-C. Wu and Y.-B. Huang, *Int. J. Pharm.*, 2008, **356**, 144–152.
- (a) H. Maeda, *Adv. Enzyme Regul.*, 2001, **41**, 189–207; (b) K. Park, S. Lee, E. Kang, K. Kim, K. Choi and I. C. Kwon, *Adv. Funct. Mater.*, 2009, **19**, 1553–1566; (c) S. Lee, J. H. Ryu, K. Park, A. Lee, S.-Y. Lee, I.-C. Youn, C.-H. Ahn, S. M. Yoon, S.-J. Myung, D. H. Moon, X. Chen, K. Choi, I. C. Kwon and K. Kim, *Nano Lett.*, 2009, **9**, 4412–4416; (d) K. H. Min, K. Park, Y.-S. Kim, S. M. Bae, S. Lee, H. G. Jo, R.-W. Park, I.-S. Kim, S. Y. Jeong, K. Kim and I. C. Kwon, *J. Controlled Release*, 2008, **127**, 208–218.
- M. de Smet, S. Langereis, S. v. den Bosch and H. Grull, *J. Controlled Release*, 2010, **143**, 120–127.
- (a) L. Paasonen, B. Romberg, G. Storm, M. Yliperttula, A. Urtti and W. E. Hennink, *Bioconjugate Chem.*, 2007, **18**, 2131–2136; (b) N. M. Khashab, M. E. Belowich, A. Trabolsi, D. C. Friedman, C. Valente, Y. Lau, H. A. Khatib, J. I. Zink and J. F. Stoddart, *Chem. Commun.*, 2009, 5371–5373.
- G. Helmlinger, A. Sckell, M. Dellian, N. S. Forbes and R. K. Jain, *Clin. Cancer Res.*, 2002, **8**, 1284–1291.
- V. Sethuraman, M. Lee and Y. Bae, *Pharm. Res.*, 2008, **25**, 657–666.
- (a) Y. Bae and K. Kataoka, *Adv. Drug Delivery Rev.*, 2009, **61**, 768–784; (b) Y. Lee, T. Ishii, Hyun J. Kim, N. Nishiyama, Y. Hayakawa, K. Itaka and K. Kataoka, *Angew. Chem., Int. Ed.*, 2010, **49**, 2552–2555.
- E. S. Lee, H. J. Shin, K. Na and Y. H. Bae, *J. Controlled Release*, 2003, **90**, 363–374.
- (a) J. Ko, K. Park, Y.-S. Kim, M. S. Kim, J. K. Han, K. Kim, R.-W. Park, I.-S. Kim, H. K. Song, D. S. Lee and I. C. Kwon, *J. Controlled Release*, 2007, **123**, 109–115; (b) X. L. Wu, J. H. Kim, H. Koo, S. M. Bae, H. Shin, M. S. Kim, B.-H. Lee, R.-W. Park, I.-S. Kim, K. Choi, I. C. Kwon, K. Kim and D. S. Lee, *Bioconjugate Chem.*, 2010, **21**, 208–213.
- M. Zeisser-Labouébe, M. Mattiuzzo, N. Lange, R. Gurny and F. Delie, *J. Drug Targeting*, 2009, **17**, 619–626.
- K. Akiyoshi, S. Deguchi, H. Tajima, T. Nishikawa and J. Sunamoto, *Macromolecules*, 1997, **30**, 857–861.
- A. Lavasanifar, J. Samuel and G. S. Kwon, *J. Controlled Release*, 2001, **77**, 155–160.
- S. Onoue, Y. Yamauchi, T. Kojima, N. Igarashi and Y. Tsuda, *Pharm. Res.*, 2008, **25**, 861–868.
- D. E. Sosnovik, E. A. Schellenberger, M. Nahrendorf, M. S. Novikov, T. Matsui, G. Dai, F. Reynolds, L. Grazette, A. Rosenzweig, R. Weissleder and L. Josephson, *Magn. Reson. Med.*, 2005, **54**, 718–724.
- K. H. Min, J.-H. Kim, S. M. Bae, H. Shin, M. S. Kim, S. Park, H. Lee, R.-W. Park, I.-S. Kim, K. Kim, I. C. Kwon, S. Y. Jeong and D. S. Lee, *J. Controlled Release*, 2010, **144**, 259–266.